

Electronic Supporting Information

Versatility and Remarkable Hypergolicity of *Exo-6, Exo-9* Imidazole-Substituted *Nido-Decaborane*

Giovanni P. Rachiero, Hatem M. Titi, Robin D. Rogers*

Department of Chemistry, McGill University, 801 Sherbrooke Street West,
Montreal, QC, H3A 0B8, Canada.

Caution! The *n*-B₁₀H₁₄ is a volatile and highly toxic solid. Never handle unsealed containers outside of a fume hood, and decontaminate all glassware and utensils that come into contact with the compounds after their utilization. Safety precautions, such as the utilization of face masks and shields, should be adopted in the ignition tests.

Materials

Imidazole (Him), and white fuming nitric acid (WFNA, 98% HNO₃) (Alfa Aesar, Ward Hill, MA, USA), 1-butylimidazole (C₄im), 1-methylimidazole (C₁im), purum kerosene, anhydrous ethyl acetate (EtOAc), tetrahydrofuran (THF), methanol (MeOH), and dry benzene (C₆H₆) (Sigma-Aldrich, Oakville, ON, Canada), 1-ethylimidazole (C₂im) (TCI, Portland, OR), *nido*-Decaborane (*n*-B₁₀H₁₄) (Santa Cruz Biotechnology, Dallas, TX, USA), absolute ethanol (EtOH) (Fischer Scientific, Ottawa, ON, Canada) and CD₃CN (Cambridge Isotope Laboratories, Tewksbury, MA, USA) were used as received.

Methods

Nuclear Magnetic Resonance (NMR). Spectra were recorded on Bruker Avance Spectrometer Bruker/Magnex UltraShield 500 MHz or 400 MHz magnet (Bruker Optics Ltd., Milton, ON, Canada) with chemical shifts reported in δ (ppm) unless noted. Spectra were collected and referenced to the solvent residual peaks for the ¹H and ¹³C, e.g. CD₃CN: δ = 1.94 ppm and δ = 118.69 ppm and 1.39 ppm, while boron trifluoride diethyl etherate (δ = 0 ppm) was used as external reference for the ¹¹B NMR. **Attenuated Total Reflection-Fourier Transform Infrared Spectroscopy (ATR FT-IR).** Spectra were recorded using a Bruker Alpha FT-IR (Bruker Optics Ltd., Milton, On, Canada) by direct measurement *via* attenuated total reflection of the neat samples on a diamond crystal. **High Resolution Mass Spectrometry (HRMS).** Spectra were recorded using atmospheric pressure chemical ionization or electro-spraying ionization on a Thermo-Scientific Exactive Orbitrap (Thermo Fischer Scientific, Waltham, MA, USA).

Thermal Gravimetric Analysis (TGA). The data were collected using a TGA5500 (TA instruments Ltd, Delaware, USA). All measurements were done under nitrogen atmosphere, in which the samples (ca. 8-12 mg) were heated to 700 °C, using a constant heating ramp of 5 °C min⁻¹ with a 30 min isotherm at 75 °C (to remove excess volatiles or residual of solvents).

Visual Melting Point Apparatus. These analyses were performed by heating open capillaries in an aluminum block with an opening which allows for visual observation. The temperature was

raised from 25 °C to 240 °C with a heating rate of ca. 10 °C min⁻¹ using a hotplate. The temperature ramp was controlled by manual timing.

Differential Scanning Calorimetry (DSC). The data were collected on a DSC2500 (TA instruments Ltd, Delaware, USA), under a stream of nitrogen. Samples (ca. 2-5 mg) were placed in hermetically sealed aluminum pans. A typical cycle included initial heating from 25 °C to the maximum temperature at a heating rate of 5 °C min⁻¹, followed by an isotherm for 5 min, cooling to -90 °C, a 10 min isotherm, and repeating the cycle twice more. Based on the results noted earlier, it was deemed unwise to collect DSC for compounds **1-3** past 100 °C. Compound **4** was studied to 160 °C to encompass the visual melting point range.

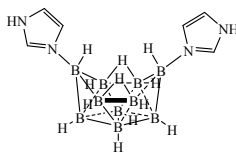
Crystallography. Single crystal X-ray diffraction (SCXRD) data were collected using a Bruker D8 Advance diffractometer with a Photon 100 CMOS area detector and an I μ S microfocus X-ray source (Bruker AXS, Madison, WI, USA). The measurements were carried out at 100(2) K on coated crystals with a thin layer of amorphous oil to decrease thermal motion effects or any structural disorder. Structure solution was carried out using the SHELXTL package from Bruker. The parameters were refined with all data by full-matrix-least-squares on F² using SHELXL. Non-hydrogen atoms were refined with anisotropic thermal parameters. Hydrogen atoms bonded to carbon were placed in calculated positions, and their coordinates and thermal parameters were constrained to ride on the carrier atom. Methyl group hydrogen atoms were refined using a riding rotating model. Hydrogen atoms bonded to boron were located from the difference map, and their positions were refined freely while their thermal parameters were constrained to ride on the carrier atom. Finally, acidic hydrogen atoms bonded to nitrogen was located from the difference map and refined as a free variable.

Intermolecular contacts and packing diagrams were made using Mercury software. Structure **1** exhibits significantly short contacts between H(δ^-)...H(δ^+) of the different neighboring molecules which are shorter than the sum of van der Waals radii (appears as alert B in CIFCheck files). Structure **2** was found to be twinned and solved in a centrosymmetric space group; other alternative transformations were not feasible.

Powder X-ray diffraction (PXRD) data was collected on a Bruker D8 Advance equipped with a Lynxeye linear position sensitive detector (Bruker AXS, Madison, WI). Neat samples were smeared directly onto the silicon wafer of a proprietary low-background sample holder. Data was collected using a continuous coupled $\theta/2\theta$ scan with Ni-filtered Cu-K α radiation.

Synthesis and Characterization of Imidazole-Substituted *n*-B₁₀H₁₄

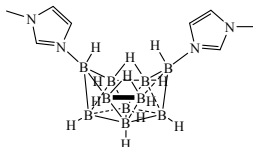
Exo-6, exo-9-(Him)₂B₁₀H₁₂ (**1**).



A 50 mL round bottom Schlenk flask was charged with Him (0.350 g, 5.1 mmol, 2.1 eq) and *n*-B₁₀H₁₄ (0.300 g, 2.45 mmol). Dry C₆H₆ was added under stirring (10 mL). The flask was purged with N₂ (3 min) and attached to a condenser. The solution was heated to 85 °C. A white solid was progressively formed. After 5 h, the oil bath was removed. The mixture was cooled to room temperature and filtered. The white solid was washed with hot C₆H₆ (6 × 10 mL). The solid was collected in a 100 mL round bottom flask and dried by rotary evaporation (T_{bath} = 50 °C, 6 h) to give **1** as a white fluffy solid (0.523 g, 2.040 mmol, 83%). ¹¹B NMR (δ , ppm): -7.81 (d, J_{BH} =

130.0 Hz), -20.32 (d, $J_{\text{BH}} = 126.2$ Hz), -22.96 (d, $J_{\text{BH}} = 112.8$ Hz), -42.39 (d, $J = 105.0$ Hz) ^1H NMR (δ , ppm): 10.87 (bs, 2H, $\Delta\nu_{1/2} = 105.7$), 8.10 (s, 2H), 7.22 (s, 2H), 7.11 (s, 2H), 1.94 (s, 2H), 1.42 (s, 4H), 0.21 (s, 2H), 0.081 (s, 2H), -4.73 (s, 2H). ^{13}C NMR (δ , ppm): 137.1, 127.2, 118.4. ATR FT-IR (cm^{-1}): 3326, 3140, 2504, 2460, 1555, 1520, 1434, 1341, 1073, 1007, 836, 736, 659, 632, 603, 448. HRMS (M^- , m/z): 255.26184, $\text{C}_6\text{H}_{19}\text{N}_4^{10}\text{B}_2\text{B}_8$; 187.22439, $\text{C}_3\text{H}_{15}\text{N}_2^{10}\text{B}_2\text{B}_8$.

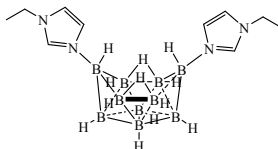
Exo-6, exo-9-(C₁im)₂B₁₀H₁₂ (2).



A 50 mL round bottom Schlenk flask was charged with *n*-B₁₀H₁₄ (0.340 g, 2.78 mmol). C₁im (0.480 g, 5.84 mmol, 2.1 eq) in dry C₆H₆ (10 mL) was added very slowly (5 min) under N₂ with stirring. A red solid precipitate in benzene was formed. The flask was attached to a condenser. The solution was heated to 85 °C. A red solid, initially observed, turned progressively to light yellow. After 5 h, the oil bath was removed. The mixture was cooled to room temperature and filtered. The solid was washed with hot C₆H₆ (6 × 10 mL), collected in a 50 mL round bottom flask, and dried by rotary evaporation ($T_{\text{bath}} = 50$ °C, 6 h) to give a yellowish solid.

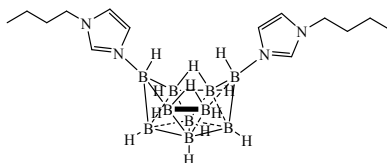
A fraction of the isolated product (0.101 g) was collected in a 25 mL round bottom flask and CH₃OH was added (10 mL). The solution was attached to a condenser and stirred at $T = 50$ °C. After 16 h, the reaction was stopped and the oil bath was removed. The solid was filtered and washed with CH₃OH (5 × 5 mL). The residue was dried by rotary evaporation ($T_{\text{bath}} = 50$ °C, 5 h) to give **2** as white solid (0.0452 g, 0.159 mmol, Yield: 45%). ^{11}B NMR (δ , ppm): -7.98 (d, $J = 118.6$ Hz), -20.31 (d, $J = 136.3$ Hz), -23.00 (d, $J = 119.7$ Hz), -42.44 (d, $J = 138.6$ Hz). ^1H NMR (δ , ppm): 8.03 (s, 2H), 7.17 (app t, 2H), 7.03 (app t, 2H), 3.70 (s, 6H), 1.94 (s, 2H), 1.40 (s, 2H), 0.15 (s, 2H), 0.068 (s, 2H), -4.76 (s, 2H). ^{13}C NMR (δ , ppm): 138.4, 127.1, 122.5, 35.6. ATR FT-IR (cm^{-1}): 3134, 3130, 2509, 2495, 2484, 2461, 1547, 1432, 1301, 1253, 1139, 1000, 849, 827, 755, 736, 698, 616, 471. HRMS (M^+ , m/z): 304.300, $\text{C}_8\text{H}_{24}\text{N}_4^{10}\text{B}_5\text{B}_5\text{Na}$.

Exo-6, exo-9-(C₂im)₂B₁₀H₁₂ (3).



Nido-B₁₀H₁₄ (0.333 g, 2.73 mmol), C₂im (0.550 g, 5.72 mmol, 2.1 eq), and dry C₆H₆ (10 mL) were combined in a procedure analogous to that for **2**. A fraction of the isolated product (0.188 g) was treated with CH₃OH (10 mL) as described for **2**. After workup, **3** was isolated as a white powder (0.112 g, 0.358 mmol, 60%). ^{11}B NMR (δ , ppm): -8.00 (d, $J = 127.1$ Hz), -20.26 (d, $J = 119.4$ Hz), -22.94 (d, $J = 114.4$ Hz), -42.42 (d, $J = 138.7$ Hz). ^1H NMR (δ , ppm): 8.08 (s, 2H), 7.18 (s, 2H), 7.10 (s, 2H), 4.04 (q, 4H, $J = 7.34$ Hz), 1.93 (s, 2H), 1.41 (t, 6H, $J = 7.30$ Hz), 0.17 (s, 2H), 0.0075 (s, 2H), -4.75 (s, 2H). ^{13}C NMR (δ , ppm): 137.4, 127.2, 120.8, 44.5, 15.7. ATR FT-IR (cm^{-1}): 3156, 3121, 2976, 2529, 2482, 1697, 1597, 1541, 1382, 1134, 1093, 998, 932, 851, 744, 692, 651, 475. HRMS (M^+ , m/z): 310.338, $\text{C}_{10}\text{H}_{28}\text{N}_4^{10}\text{B}_4\text{B}_6$.

Exo-6, exo-9-(C₄im)₂B₁₀H₁₂ (4).



Nido-B₁₀H₁₄ (0.301 g, 2.46 mmol), C₄im (0.642 g, 5.17 mmol, 2.1 eq), and dry C₆H₆ (10 mL) were combined in a procedure analogous to that for **2**. A fraction of the isolated product (0.0554 g) was treated with CH₃OH (10mL) as described for **2**. After workup, **4** was isolated as a white powder (0.0351 g, 0.0952 mmol, 63%). ¹¹B NMR (δ, ppm): -7.93 (d, *J* = 122.1 Hz), -20.31 (d, *J* = 113.1 Hz), -22.91 (d, *J* = 102.6 Hz), -42.41 (d, *J* = 135.6 Hz). ¹H NMR (δ, ppm): 8.07 (app t, 2H), 7.18 (app t, 2H), 7.09 (t, 2H, *J* = 1.62 Hz), 3.99 (t, 4H, *J* = 7.28 Hz), 1.92 (s, 2H), 1.76 (q, 4H, *J* = 14.8 Hz), 1.41 (s, 2H), 1.29 (sext, 4H, *J* = 7.61 Hz), 0.92 (t, 6H, *J* = 14.8 Hz), 0.17 (s, 2H), 0.0076 (s, 2H), -4.75 (s, 2H). ¹³C NMR (δ, ppm): 137.7, 127.2, 121.2, 49.1, 32.8, 20.1, 13.6. ATR FT-IR (cm⁻¹): 3141, 2956, 2927, 2871, 2506, 2458, 1540, 1453, 1132, 1097, 998, 829, 745, 687, 648, 463. HRMS (M⁺, *m/z*): 366.401, C₁₄H₃₆N₄¹⁰B₄B₆.

Thermal Degradation Analysis

TGA data were collected for compounds **1-4** (Fig. S1, left). The complicated TGA traces confirm multiple transitions for these materials. Although the 5% onset of decomposition temperatures (*T*_{5% onset}) were quite high (644 °C for **1**, 224 °C for **2**, 384 °C for **3** and 328 °C for **4**), it was clear that each had a first decomposition step in the range of 160-200 °C (Fig. S1, right). This is consistent with degradation accompanied by a progressive loss of molecular hydrogen as found by Rozenberg *et al.* for the decaborane diammoniate.¹

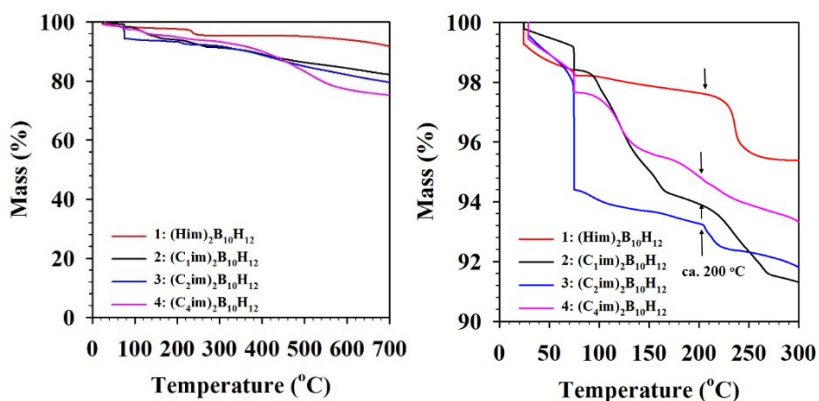


Fig. S1: TGA and regions of decomposition of **1-4**

Visual Observations on Heating

Compounds **1** and **2** did not appear to melt; **1** changed color while for **2** the color variation was less appreciable (Table S1). On the other hand, **3** appeared to melt with decomposition at 190-200 °C. The longest alkyl chain derivative **4** was unique where at 130-140 °C it did melt forming a colorless liquid, which eventually decomposed (turning yellow) at ca. 190-200 °C.

Table S1. Visual melting points of 1-4

Compound	Melting/Decomposition	Observations
1 (Him) ₂ B ₁₀ H ₁₂	N/A	Changed color at ca. 200-210 °C from white to greenish
2 (C ₁ im) ₂ B ₁₀ H ₁₂	N/A	Less appreciable modification of color
3 (C ₂ im) ₂ B ₁₀ H ₁₂	190-200 °C	Melts with decomposition with variation from white to yellow
4 (C ₄ im) ₂ B ₁₀ H ₁₂	130-140 °C	Melts to a colorless liquid; turned to yellow at ca. 190-200 °C

The progressive heating of **1-4** is accompanied by a clear modification of the color in **1**, while for **2** the variation of color was less clear at the visual analysis. The chromatic variation in **1** and **2** in combination with the TGA results suggest progressive degradation. Both **3** and **4** melt without variation of the color for the latter, while **3** turns yellow at ca. 200 °C suggesting decomposition as noted in the TGA.

To confirm the decomposition reactions noted above, PXRD data was collected on **1** before and after heating in an open vial to 100 or 250 °C. For comparison, the TGA data for **1** are shown in Fig. S2, left. The diffractograms (Fig. S2, right) confirm no changes to **1** after heating to 100 °C, but the formation of an amorphous solid after heating to 250 °C.

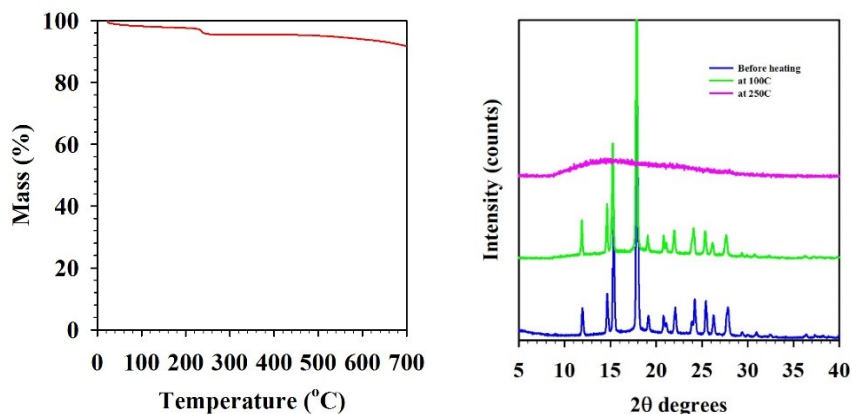


Fig. S2: TGA and PXRD of 1.

In addition, significant changes were observed in the FT-IR of **1** (Fig. S3) after heating to 100 °C or 250 °C, where the B-H stretches usually located at 2499 and 2460 cm⁻¹, essentially disappeared. The symmetric and asymmetric B-B stretches usually at ca. 829 cm⁻¹ and 1067 cm⁻¹, respectively, also exhibited major changes.² These stretches shifted to 791 and 1051 cm⁻¹, respectively, indicating possible rearrangement of the decaborane cluster or degradation. The disappearance of the imidazole N-H stretches at 3327 cm⁻¹ is a sign of the decomposition or loss

of the imidazole ring. Here, the acidic protons of the imidazole and N-H may have reacted with the hydrogen of the boron cluster as found for diammoniate ligands.⁴ Finally, new broad stretches were also found and these could be assigned as B-O bonds (usually appearing as a broad peak at ca. 1310 cm^{-1}), due to the reaction with the O_2 in the air.

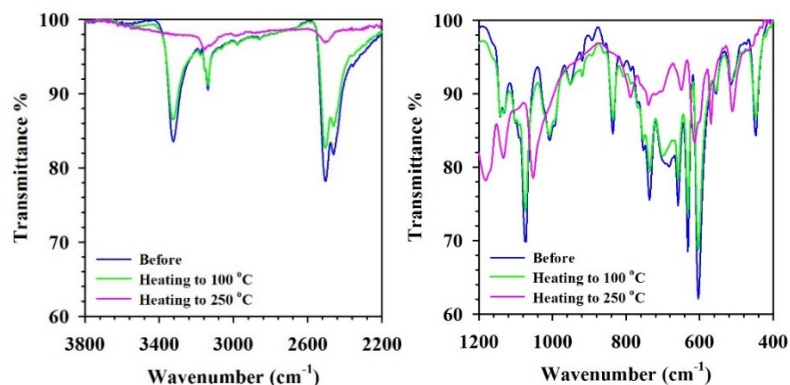


Fig. S3: IR of 1

Differential Scanning Calorimetry (DSC)

DSC data (Fig. S4) on 1-3 confirmed no thermal events below 100 °C . Compound 4, however, exhibited two endotherms at $T_{m\ peak} = 130.26\text{ °C}$ ($T_{m\ onset} = 126.77\text{ °C}$) and $T_{m\ peak} = 153.47\text{ °C}$ ($T_{m\ onset} = 151.38\text{ °C}$), an exotherm at 137.22 °C , a glass transition on the second and third cycles at 24.82 °C (see ESI†). Compound 4 appears to go through a first melt, solid-to-solid transition, and a second melt.

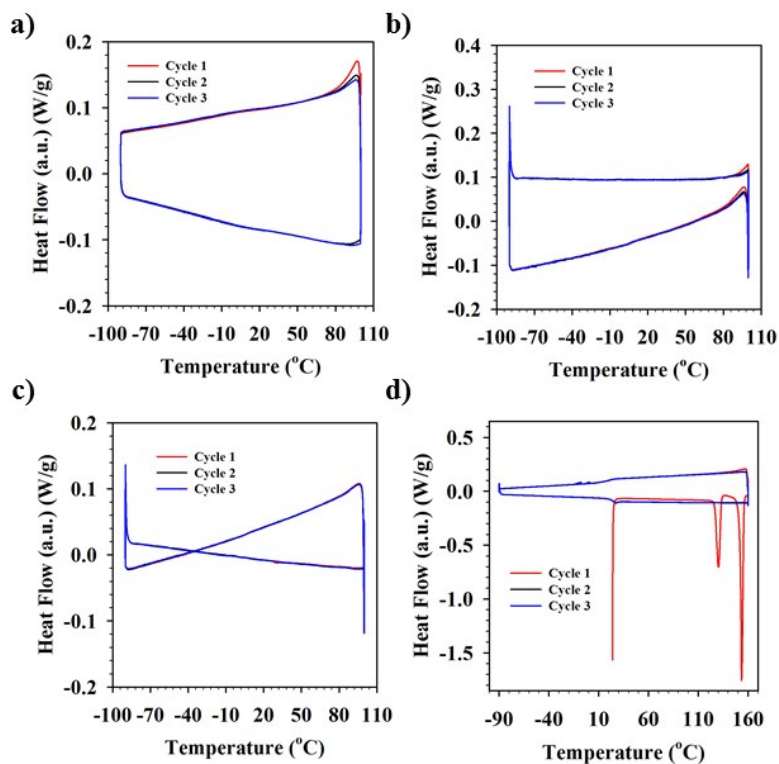


Fig. S4: DSC of 1 (a), 2 (b), 3 (c), and 4 (d)

Crystallization of Imidazole-Substituted n -B₁₀H₁₄

Typical procedure for crystallization. The compound **1** (ca. 0.005 g) was dissolved with CH₃CN (1 mL) in a vial. The solution was sonicated (10 min) and layered with C₆H₆ (1 mL). After two days, colorless block crystals suitable for single crystal X-ray analysis were obtained. Analogous procedures were applied to **2-4** with identical results. Colorless, block crystals of the compound [C₄Him][B₅O₆(OH)₄] (**5**), were isolated from a THF solution of **4** layered with C₆H₆.

Table S2. Crystal data and structure refinement for **1-5**

	1	2^a	3	4	5
Formula	C ₆ H ₂₀ B ₁₀ N ₄	C ₈ H ₂₄ B ₁₀ N ₄	C ₁₀ H ₂₈ B ₁₀ N ₄	C ₁₄ H ₃₆ B ₁₀ N ₄	C ₇ H ₁₇ B ₅ N ₂ O ₁₀
Fw	256.50	284.41	312.46	368.57	343.27
Crystal system	Monoclinic	Monoclinic	Orthorhombic	Monoclinic	Triclinic
Space group	<i>P</i> 2 ₁ / <i>n</i>	<i>P</i> 2 ₁ / <i>n</i>	<i>P</i> bcn	<i>P</i> <i>n</i>	<i>P</i> -1
a [Å]	7.2587(12)	7.4298(6)	10.0069(8)	10.4108(7)	9.1839(7)
b [Å]	13.5938(19)	13.7626(14)	13.2066(10)	8.2731(6)	9.3861(7)
c [Å]	14.524(2)	16.0828(17)	14.6031(12)	12.8841(8)	9.7709(8)
α [°]	90	90	90	90	73.615(3)
β [°]	96.947(6)	100.902(3)	90	92.532(2)	86.252(3)
γ [°]	90	90	90	90	69.954(3)
V [Å³]	1422/6(4)	1614.8(3)	1929.9(3)	1108.62(13)	758.64(10)
Z	4	4	4	2	2
ρ_{calcd} [mg m⁻³]	1.1968	1.170	1.075	1.104	1.503
μ [mm⁻¹]	0.064	0.062	0.057	0.059	0.129
F(000)	536.1	600.0	664.0	396.0	356.0
2θ range [°]	5.66 to 55.32	5.92 to 55.098	5.108 to 62.54	4.924 to 53.536	4.724 to 54.31
Refl. collected	28004	31587	39969	21717	12744
Refl. unique	3264	3705	3129	4568	3358
R(int)	0.1793	0.0797	0.0627	0.0364	0.0517
Goodness-of-fit on F²	1.027	1.179	1.050	1.032	1.010
R_{sigma}	0.0992	0.0451	0.0288	0.0278	0.0432
Restraints/parameters	0/180	0/201	0/111	2/255	0/222
R₁ [I > 2σ(I)]	0.0666	0.0865	0.0439	0.0337	0.0628
wR₂ [I > 2σ(I)]	0.1311	0.2195	0.1204	0.0830	0.1674
R₁ [all data]	0.1350	0.0982	0.0529	0.0366	0.0879
wR₂ [all data]	0.1563	0.2248	0.1272	0.0844	0.1846
± Δρ_{max} [e Å⁻³]	0.63/-0.53	0.49/-0.36	0.44/-0.35	0.15/-0.20	0.77/-0.44

^a Twinned crystals

The compound **1**, (Him)₂B₁₀H₁₂, crystallizes in the monoclinic space group *P*2₁/*n* and the asymmetric unit contains one unique entity. Significant short H^(δ-)...H^(δ+) contacts occur between the adjacent entities through the protons of *N*-13 and *N*-19 of the imidazole rings and the adjacent hydrogen atoms of the boron hydride cluster led to the formation of 1D non-covalent chains. Due to directionality and strength of these non-covalent interactions, the molecules are arranged in 2D-

like sheets held together by Coulombic forces across the lattice (**Fig. S5**). Noteworthy, the imidazole rings are slightly tilted from a perfect eclipsed position with a $C-15/N-11/N-16/C-17$, that reduces the symmetry of the cluster along with the position of the protonated N atoms.

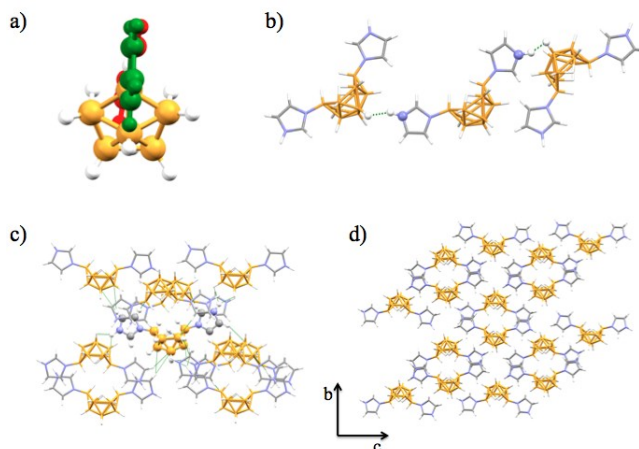


Fig. S5: Illustration of the environment of **1** with the tilted dihedral angle of the imidazole rings in red and green (*a*). The dashed lines in (*b*) represent the short $H^{(\delta^-)}\cdots H^{(\delta^+)}$ contacts and the involved H and N atoms are presented in white and blue sphere, respectively. The crystal packing is shown in (*c*) and (*d*).

The compound **2**, $(C_1im)_2B_{10}H_{12}$, crystallizes in the monoclinic space group $P2_1/n$. In the structure, the methyl groups are oriented in the same direction with respect to the cluster (**Fig. S6**). These arms are forming a wide range of $H^{(\delta^-)}\cdots H^{(\delta^+)}$ contacts between the imidazole functionalities and the hydrogen atoms of the adjacent clusters that produce 1D Coulombic based chains along the lattice. In addition, $C-H\cdots\pi$ interactions between the imidazolium moieties also assist in stabilizing the formation of formed chains. All this led to a “crowded” environment around each entity with nine neighboring boron hydride species. Interestingly, the packing shows isolation columns between the entities, where the imidazole rings are separating the entities along the c -axis.

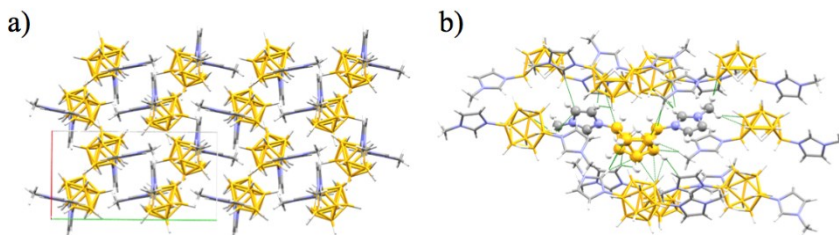


Fig. S6: Crystal packing of **2** (*a*) and the molecular environment (*b*).

The compounds **3** and **4**, $(C_2im)_2B_{10}H_{12}$ and $(C_4im)_2B_{10}H_{12}$, crystallize in the orthorhombic ($Pbcn$) and monoclinic (Pn) space groups, respectively. The asymmetric unit of **3** contains one half of the substituted boron cluster, while the core of the boron hydride species is located on a 2-fold axis. The asymmetric unit shows only one unique entity of **4**, the butyl chains are oriented perpendicularly with respect to the imidazole ring. Each molecule in **3** and **4** is surrounded by ten and fourteen, respectively, other neighboring entities through a series of short contacts (**Fig. S7** and **S8**). Interestingly, in both structures most of these contacts are based on $H^{(\delta^-)}\cdots H^{(\delta^+)}$

interactions, generated by the ethyl and butyl groups. Moreover, a unique bridging μ -hydrogen atom interacts with a hydrogen in the α position for in the alkyl chain of the neighboring cluster.

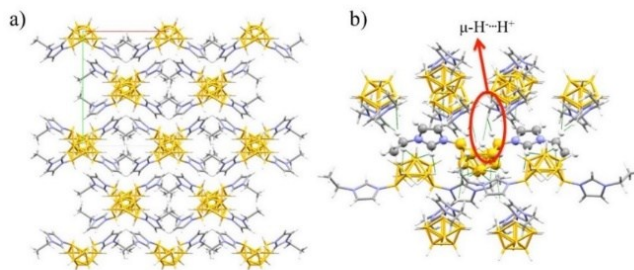


Fig. S7: Crystal packing of **3** (a) and the molecular environment (b). Note the short contacts between the bridging μ -hydrogen atom and the δ^+ of the H atoms of the adjacent molecules.

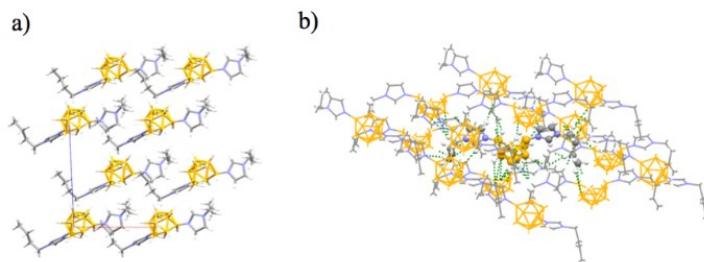


Fig. S8: Crystal packing of **4** (a) and the molecular environment (b).

The geometry of the boron-clusters of **1-4** is preserved in all structures with slight variations for the distances of the B-B atoms (1.729(3)-1.886(4) Å for **1**, 1.739(4)-1.874(5) Å for **2**, 1.743(1)-1.880(1) Å for **3**, and 1.737(3)-1.884(1) Å for **4**) in comparison with an analogous diamino-decaborane (1.729(4)-1.868(3) Å).³ All B-B-B angles in **1-4** were found to be in good agreement with the diamino-decaborane skeleton. The B-N distances are 1.550(3) Å and 1.553(3) Å for **1**, 1.551(4) Å and 1.562(4) Å for **2**, 1.554(1) Å for **3**, and 1.559(3) Å and 1.563(3) Å for **4**. The attractions between the hydrogen atoms of the cluster and the δ^+ hydrogen of the imidazole rings lead to tight crystal packing. Different computational evaluations especially for simpler systems such as BH_3NH_3 show that the aggregation is influenced by dipole-dipole interactions, suggesting a correlation with our systems.⁴

A molecular overlay of **1-4** demonstrates that **1** has an eclipse-like conformation with a torsion angle of 6.3° (**Fig. S9**), while **2-4** display staggered-like conformations with torsion angles of 84.2° , 87.2° and 76.0° , respectively. The packing of **3**, which has the largest torsion angle and led for the separation of the boron clusters along the lattice causing lower stability.

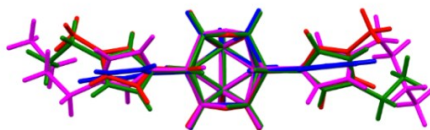


Fig. S9: Overlay of **1-4** (view from top) reveals the tilted conformation of the related imidazole rings. Compounds **1-4** are depicted in blue, red, green, and purple, respectively.

The Kitaigorodskii-type packing index (KPI)⁵ was calculated using a PLATON package⁶ to evaluate the influence of the alkyl chains on the stability of the crystal packing. It should be noted that structures have a typical packing index in order of 65%. The calculation shows that all the crystal structures are in good agreement with the KPI for **1**, **2**, and **4** with values of 68.9%, 69.0%, and 67.3%, respectively. The KPI value slightly decreases for **3** (64.2%) due to the larger torsion angle which separates the layers in the crystal packing. Unlike **3**, it seems that **4** has tighter crystal packing owing this stability to a smaller torsion angle and wider range of intermolecular interactions.

The compound **5** isolated from a THF solution of **4** layered with C₆H₆, crystallizes in the triclinic space group *P*-1. The environment around each anion is surrounded by six anions and seven cations, while each cation's environment is occupied by one cation and seven anions. The ionic species are engaged in a series of hydrogen bonds between the protonated N atoms of the imidazolium ring and the O atom of the heterocyclic pentaborate rings. The hydroxyl groups form a 3D grid-like arrangement and their 1D channels are occupied by the cation entities (**Fig. S10**).

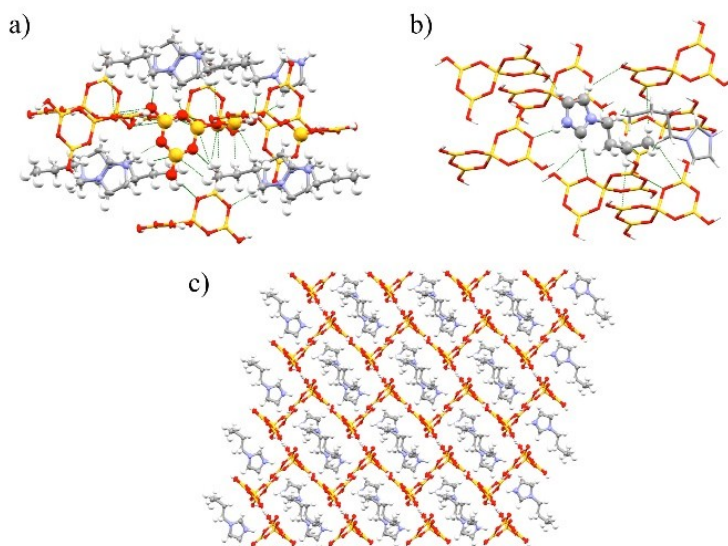


Fig. S10: Molecular environment of the anion (*a*), cation (*b*), and crystal packing along the *a*-axis (*c*).

Solubility and Hypergolic Tests

Solubility Tests. An aliquot of **1-4** (ca. 0.002-0.004 g) was weighed in 5-mm NMR tube and the solvent was added (0.7 mL). The mixture was sonicated (2 min). ¹H NMR spectra were recorded by a multiple site presaturation pulse sequence with 100 ms NOESY mixing time to suppress the solvent peaks, a 25 s recycle delay, and a value of 80.6 for the receiver gain in the presence of MeOH, EtOH, THF, and EtOAc and 36.0 with Kerosene. The NOESY sequence ensures a good suppression of the solvent and a flat baseline, however, all spectra were still baseline corrected before integration. Concentrations were calculated using the ERETIC 2 routine as implemented in Bruker TopSpin 3.5 pl 6,⁷ utilizing a solution of sucrose 2.00 mM in 90% H₂O + 10% D₂O as the external standard. The integration focused on the aromatic protons of the imidazoles which have the advantage of not overlapping with the suppressed region.

Hypergolic Tests with the Compounds. An aliquot of **1-4** (ca. 0.005 g) was treated with WFNA by a typical drop test: A single drop (10 μL) of acid was added via a 100 μL Hamilton syringe (Hamilton, Reno, NV, USA) from a fixed height (5 cm) onto a 4.5 cm vial containing the sample. A Redlake MotionPro Y4 (Tallahassee, FL, USA) high speed CCD camera at 1000 frames/s was utilized to monitor the ignition. The ignition delay was measured as the time in milliseconds for ignition to occur after the initial contact of fuel and oxidizer. The test was replicated three times, the values for ignition delay were averaged, and the standard deviation was calculated.

Hypergolic Test in Molecular Solvents (Mixtures). An aliquot of **1-4** (ca. 0.003 g) was weighed in a 4.5 cm vial and the solvent (90 μL) was added. The vial was closed, the mixture was agitated by a laboratory vortex (3200 rpm, 3 min) and then left at room temperature (15 min). WFNA (5 drops, $5 \times 10 \mu\text{L}$) was added via a 100 μL Hamilton syringe from a fixed height (5 cm) onto a 4.5 cm vial containing the sample. A Redlake MotionPro Y4 high speed CCD camera at 1000 frames/s was utilized to monitor the ignition. Each drop of the oxidizer released from the syringe splashed on the surface of the mixture with simultaneous contact of solid and liquid. The test for each compound was performed only once.

Hypergolic Test in Molecular Solvents (Homogeneous Solutions). A 10 cm vial was charged with **2** (0.0033 g). Kerosene (0.7 mL, $n_{\text{solute}}/n_{\text{solvent}} = 0.14 \times 10^{-4}$) was added. The vial was closed, the mixture was stirred using a laboratory vortex (3200 rpm, 3 min) and then left at room temperature for 15 min. The mixture was filtered with a circular disc membrane for syringes (VWR, 0.45 μm , PTFE membrane) to ensure isolation of the homogeneous solution. The test for hypergolic ignition was carried out by two different procedures: **a-** A 4.5 cm vial was charged with the homogeneous solution kerosene-(C₁im)₂B₁₀H₁₂ (90 μL). Five drops of WFNA ($5 \times 10 \mu\text{L}$) were added via a 100 μL Hamilton micro syringe into the vial containing the solution from a fixed height (5 cm). **b-** A 4.5 cm vial was charged with WFNA (90 μL). Five drops of homogeneous solution kerosene-(C₁im)₂B₁₀H₁₂ ($5 \times 10 \mu\text{L}$) were added via a 100 μL Hamilton micro syringe into the vial containing the acid from a fixed height (5 cm). Identical procedures were carried out using **2** (0.0022 g) in MeOH (0.7 mL, $n_{\text{solute}}/n_{\text{solvent}} = 0.219 \times 10^{-4}$). The same procedure described above were adopted in the experiments with **4** utilizing, respectively, 0.0035 g and 0.0021 g of the compound, respectively, in kerosene (0.7 mL, $n_{\text{solute}}/n_{\text{solvent}} = 0.138 \times 10^{-4}$) and in MeOH (0.7 mL, $n_{\text{solute}}/n_{\text{solvent}} = 0.223 \times 10^{-4}$). The test for each compound was performed only once.

Table S3. Ignition Delays (IDs, ms) for hypergolic tests of **1-4** in molecular solvents^{a,b,c,d,e}

Compound	MeOH		EtOH		THF		EtOAc		Kerosene	
	– ^e		– ^e		– ^e		ID ₁ : 14	ID ₂ : –	ID ₁ : 35	ID ₂ : 126
1, (Him)₂B₁₀H₁₂	No flames, only smoke was observed		No flames, only smoke was observed		No flames, only smoke was observed		<i>First drop:</i> Discontinuous flame (ca. 2 cm) Duration: ca. 20 ms <i>Second drop:</i> No flames, only smoke was observed		<i>First drop:</i> Discontinuous flame (ca. 1 cm) Duration: ca. 15 ms <i>Second drop:</i> Continuous flame (ca. 5 cm) Duration: ca. 30 ms.	
2, (C₁im)₂B₁₀H₁₂	ID ₁ : 47	ID ₂ : 1	ID ₁ : 8	ID ₂ : 25	ID ₁ : 4	ID ₂ : 2	– ^e		ID ₁ : 31	ID ₂ : 109
	<i>First drop:</i> Continuous flame (ca. 3 cm) Duration: ca. 1150 ms <i>Second drop:</i> Continuous flame (ca. 1.5 cm) Duration: ca. 350 ms		<i>First drop:</i> Continuous flame (ca. 6 cm) Duration: ca. 20 ms <i>Second drop:</i> Discontinuous flame (< 0.5 cm) Duration: ca. 30 ms		<i>First drop:</i> Continuous flame (ca 7 cm) Duration: ca. 50 ms <i>Second drop:</i> Continuous flame (ca 7 cm) Duration: ca. 50 ms		No flame. Only smoke was observed.		<i>First drop:</i> Discontinuous flame (ca. 2 cm) Duration: ca. 70 ms <i>Second drop:</i> Continuous flame (ca. 2.5 cm) Duration: ca. 40 ms.	
3, (C₂im)₂B₁₀H₁₂	ID ₁ : 5	ID ₂ : –	ID ₁ : –	ID ₂ : 2	– ^e		– ^e		ID ₁ : –	ID ₂ : 564
	<i>First drop:</i> Discontinuous flame (ca. 0.5 cm) Duration: ca. 15 ms Combustion of flammable vapors; ignition with a visible flame (ca. 3 cm) for ca. 8 ms <i>Second drop:</i> No flames, only smoke was observed		<i>First drop:</i> No flames, only smoke was observed <i>Second drop:</i> Continuous flame (ca. 0.5 cm) Duration: ca. 25 ms.		No flames. Only smoke was observed		No flames, only smoke was observed		<i>First drop:</i> No flames, only smoke was observed <i>Second drop:</i> Discontinuous flame (ca. 2 cm) Duration: ca. 20 ms	
4, (C₄im)₂B₁₀H₁₂	ID ₁ : 8	ID ₂ : –	ID ₁ : 128	ID ₂ : –	– ^e		– ^e		ID ₁ : 4	ID ₂ : –
	<i>First drop:</i> Discontinuous flame (ca. 0.5 cm) Duration: ca. 15 ms Combustion of flammable vapors; ignition with a visible flame (ca. 2 cm) for ca. 10 ms <i>Second drop:</i> No flames, only smoke was observed		<i>First drop:</i> Discontinuous flame (ca. 0.2 cm) Duration: ca. 3 ms Combustion of flammable vapors; ignition with a visible flame (3 cm) for ca. 5 ms <i>Second drop:</i> No flames, only smoke was observed		No flames, only smoke was observed		No flames, only smoke was observed		<i>First drop:</i> Discontinuous flame (ca. 2 cm) Duration: ca. 30 ms <i>Second drop:</i> No flames, only smoke was observed.	

^a The IDs for the 1st and 2nd drop; ^b When observed, the color of flames was white with green accents; ^c A solid and a liquid was left after addition of the oxidizer; ^d The flame was extinguished before the contact of the second drop of oxidizer; ^e –: No ignition.

References

- ¹ A. S. Rozenberg, G. N. Nechiporenko and A. P. Alekseev, *Russ. Chem. Bull.*, 1978, **27**, 284.
- ² L. J. Bellamy, W. Gerrard, M. F., Lappert and R. L. Williams, *J. Chem Soc.*, 1958, **481**, 2412.
- ³ S. Mebs, R. Kalinowski, S. Grabowsky, D. Förster, R. Kickbusch, E. Justus, W. Morgenroth, C., Paulmann, P. Luger, D. Gabel and D. Lentz, *Inorg. Chem.*, 2011, **50**, 90.
- ⁴ G. Merino, V. I. Bakmutov and A. Vela, *J. Phys. Chem. A* 2002, **106**, 8491.
- ⁵ P. van der Sluis and A. L. Spek, *Acta Cryst.* 1990, **A46**, 194.
- ⁶ A. L. Spek, *Acta Cryst.* 2009, **D65**, 148.
- ⁷ (a) G. Wider and L. Dreier, *J. Am. Chem. Soc.*, 2006, **128**, 2571; (b) D. I. Hoult and R. E. Richards, *J. Magn. Reson.*, 1976, **24**, 71; (c) D. I. Hoult, *Concepts in Magn. Reson.*, 2000, **12**, 173.